

A Neural Network Framework to Retrieve Material Properties From Displacement Data

by

Tina Hajinejad

A report
presented to the University of Waterloo
in fulfillment of the
research paper requirement for the degree of
Master of Mathematics
in
Computational Mathematics

Waterloo, Ontario, Canada, 2024

© Tina Hajinejad 2024

Author's Declaration

I hereby declare that I am the sole author of this thesis. This is a true copy of the thesis, including any required final revisions, as accepted by my examiners.

I understand that my thesis may be made electronically available to the public.

Abstract

In this research, we introduce a neural network method as a preliminary step towards our ultimate goal of identifying the parameters of complex structures, such as bio-molecules, under environmental conditions.

By employing a simplified truss framework, we aim to explore the elastic responses of structures subjected to thermal environmental fluctuations. This method simplifies the complexities into models composed of rod elements and nodes, which experience deformation and movement due to thermal noise.

The displacement of nodes, crucial for understanding the system's dynamics, is determined by the modulus of elasticity and the cross-sectional area (EA) of the rods. To estimate these varying EA values across the model, we utilize a fully connected neural network trained with simulated data, thereby enhancing our ability to predict the structure's behavior under various conditions.

This technique offers a way of investigating the elastic characteristics of systems, providing valuable insights into their dynamic behavior without specifying their biological or molecular nature. The ultimate purpose of our work is to enable the recovery of material properties from experimental data, such as those obtained from cryo-electron microscopy (cryo-EM) experiments, further bridging the gap between theoretical models and practical, observable phenomena.

Acknowledgements

I'd like to thank my supervisors, Professor Stephen Vavasis and Katerina Papoulia, for their guidance through this process.

Thanks also to Sarah Harris and Molly Gravett from the University of Leeds for their support and for answering our questions.

Dedication

This is dedicated to my dear sister, Bahar, whose unwavering support kept me going through this program.

Table of Contents

Author's Declaration	ii
Abstract	iii
Acknowledgements	iv
Dedication	v
List of Figures	viii
1 Introduction	1
1.1 Background	1
1.2 Challenges with bio-molecular modeling	2
1.3 Cryo-Electron Microscopy	2
1.4 Material Properties	3
1.5 Neural Networks	4
1.6 Forward Euler algorithm	5
1.7 Truss model	7
1.8 Ergodic Hypothesis	8

2	Procedure	11
2.1	An Example Truss Model	11
2.2	Data Generation	14
2.3	The Neural Network	14
2.4	The Training process	16
3	Results	18
4	Future Work	20
	References	22

List of Figures

1.1	The image showcases GroEL protein complexes from a frozen-hydrated specimen, highlighting how these complexes can be seen in different orientations relative to the electron beam (Milne et al., 2013)	4
1.2	Image retrieved from https://medium.com/data-science-365/overview-of-a-neural-networks-learning-process-61690a502fa	6
1.3	A simple truss (Alderliesten, 2022)	8
1.4	(a) Cryo-EM map of My05a-S1-6IQ (Gravett, 2022) (b) Nodes in mesh closest to vector coordinates in Cryo-EM model (Gravett, 2022)	9
2.1	(a) The simplified Truss structure in 2D. (b) The simplified Truss structure in 3D. The elements colored red have less flexibility than the blue elements. Each data point in a particular histogram corresponds to the two extremal eigenvalues of the all-pairs squared distance matrix of the truss model at a particular time step during simulation. A new data point is inserted in the histogram every 1000 time steps.	13
2.2	EA 1e-5	15
2.3	EA 1e-6	15
2.4	EA 1e-8	15
2.5	EA 1e-9	15
2.6	Cross validation MSE (Mean Squared Error) to choose the optimum number of neurons of the hidden layer.	17
2.7	The training process with piece-wise learning rate and validation tolerance of 5.	17

3.1	The Predicted vs. Actual values of Test data. The blue and red dots show the two targets and the red line shows the line of perfect prediction.	19
-----	---	----

Chapter 1

Introduction

1.1 Background

Cytoskeletal motors, crucial for various cell processes such as transport, movement, cell division, and growth, function as mechanoenzymes. They convert the chemical energy of ATP into mechanical force. ATP, the primary energy carrier within the cell, captures chemical energy from food molecule breakdown and releases it to fuel other cellular processes. In essence, ATP is the cell's energy currency, powering vital functions like active transport, muscle contraction, and chemical synthesis[<https://unitedmedicines.com/adenosine-triphosphate/>].

Unlike larger motors, nanoscale motors are heavily impacted by their viscous environment, as well as thermal fluctuations and Brownian motion (Purcell, 1977; Bustamante et al., 2001). Their ability to operate in these conditions, along with their vital role in cellular activities, highlights the importance of studying their mechanical properties in biology, physics, and engineering (Bustamante et al., 2001; Nelson et al., 2010; Hess, 2011; Robert-Paganin et al., 2020).

Modeling proteins like myosin is essential for understanding the movement of proteins in a cell with precision. This, in turn, is important because, through this movement, proteins transport cargo through the cell. The problem is very similar to mechanical devices operating at the nanoscale. However, typical motions experienced by standard machines in our typical environment, myosin, and other proteins operate in a viscous liquid environment and are subject to random thermal forces. Thus, by studying how myosin responds to thermal fluctuations—whether it takes short steps, adjusts to the loads, or

can keep itself moving in such unpredictable surroundings—we build our understanding of its mechanical efficacy and resilience. This data is crucial for effectively implementing advanced material technologies and devices (Gravett, 2022).

1.2 Challenges with bio-molecular modeling

Many existing bio-molecular modeling techniques, such as conventional atomistic simulations, require the detailed atomic structure as input, limiting their applicability to molecules with higher-resolution structural information, which is often unavailable. This highlights the necessity for alternative modeling approaches that can accommodate less detailed structural data while still providing valuable insights.

The development of lower-resolution experimental techniques, such as SAXS, cryo-electron microscopy, fluorescent resonance energy transfer labeling, ion-mobility mass-spectroscopy, and atomic force microscopy have begun to offer dynamic information at the mesoscopic level. These advancements provide new opportunities to study bio-molecular flexibility and dynamics using computational models that can integrate with experimental data.

Based on the discussion above, it is clear that we need computational approaches that can provide precise material characteristics for individual bio-molecules, using data from experiments. This way, we can start to compare how flexible these bio-molecules are, considering their unique shapes. Understanding this flexibility is key, especially when we're looking at molecules like molecular motors that are constantly moving. This kind of insight is crucial for unraveling how these molecules work and what they do in the cell.

1.3 Cryo-Electron Microscopy

“Cryo-Electron Microscopy” (Milne et al., 2013), often abbreviated as “cryoEM”, has evolved in the past decades to encompass a wide range of experimental techniques. Fundamentally, each of these methods relies on the concept of imaging specimens sensitive to radiation using a transmission electron microscope, while the specimens are kept at cryogenic temperatures.

In the field of biology, cryo-EM is a powerful tool that enables us to look at a variety of structures, from intact whole tissues and frozen cells to tiny bacteria, viruses,

and protein molecules. It includes specializations such as cryo-electron tomography, single-particle cryo-electron microscopy, and electron crystallography. These methods have been used successfully to study biological structures under different conditions. They can be utilized on their own or mixed with other methods, like X-ray crystallography and NMR spectroscopy. This way, researchers get a fuller picture of what these structures look like and how they work.

So why is it not routinely possible to image individual proteins, viruses and cells in their natural state directly under an electron microscope at atomic resolution? The main reason for this is the extensive damage caused by the interaction between electrons and organic matter. Electron irradiation leads to the breaking of chemical bonds and the formation of free radicals, which in turn cause more secondary damage.

Modern "high-resolution" electron microscopy uses two approaches to solve this problem. One approach involves "cryo-electron microscopy", in which frozen samples are used for imaging, kept at the temperature of either liquid nitrogen or liquid helium.

The development of methods to rapidly freeze (vitrify) biological specimens within a layer of glass-like ice, which could then be imaged at liquid nitrogen and/or helium temperatures, led extensive use of this approach.

Perhaps the most commonly used variant of cryo-electron microscopy is single-particle analysis. In this technique, data from a large number of 2D projection images showing identical copies of the protein complex in different orientations are combined with a 3D reconstruction of the structure. When atomic models are available for some or all of the sub-components of a complex, they can be placed or fitted onto a density map to produce pseudo-atomic models, which greatly expands the information available from electron microscopy. Figure 1.1 shows an example Cryo-EM image.

1.4 Material Properties

The Fluctuating Finite Element Analysis (FFEA) model addresses the challenge of simulating large bio-molecules by treating them as three-dimensional objects. This approach is very useful for biological systems for which large-scale motions are more important than the chemical interactions. The model is suitable for representing globular structures, like certain parts of the Ndc80C protein complex, suggesting the importance of understanding material properties to grasp the functional dynamics of these bio-molecules. However, it is known that 3D continuum methods face limitations in accurately representing slender, elongated structures such as the coiled-coil region of Ndc80C because of the difficulties in

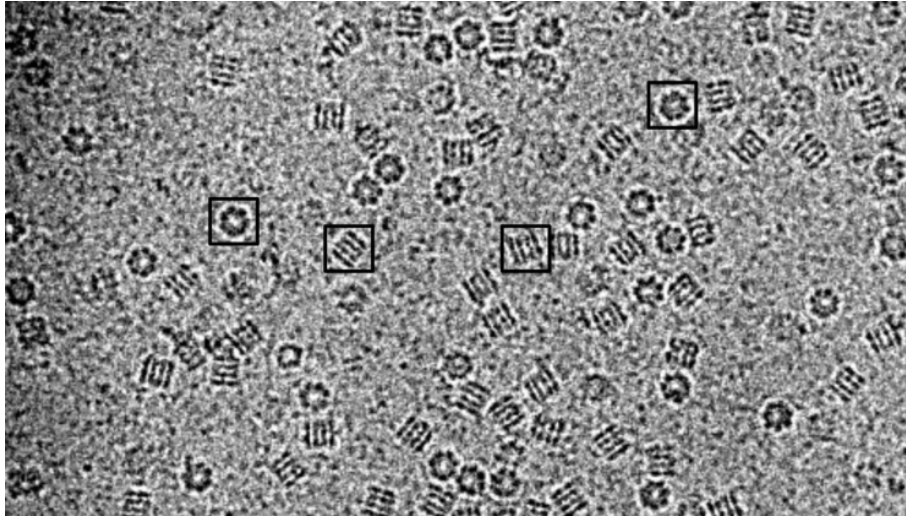


Figure 1.1: The image showcases GroEL protein complexes from a frozen-hydrated specimen, highlighting how these complexes can be seen in different orientations relative to the electron beam (Milne et al., 2013)

capturing the correct thermal fluctuations at the small length scales involved (Welch et al., 2020).

To effectively model slender biological structures such as alpha-helices, understanding their material properties becomes essential (Welch et al., 2020). We can gain crucial insights into their behaviors by developing models that account for how these bio-molecules can stretch, bend, and twist. This knowledge is key to comprehending how these molecules function within cells, highlighting the importance of material properties in the study of bio-molecular movement and functionality.

1.5 Neural Networks

Neural networks are computational models inspired by structure and function of the human brain. They consist of layers of nodes, or "neurons," connected to allow them to learn and make decisions from input data. By adjusting the connections between these nodes during training, neural networks can identify patterns, classify data, and predict outcomes for a wide range of problems, making them incredibly versatile tools in artificial intelligence and machine learning.

Neural networks can be beneficial in material property retrieval using cryo-electron microscopy (cryo-EM) images. Cryo-EM images provide detailed views of biological structures, from entire tissues to individual protein molecules, often at resolutions that challenge traditional analysis methods. By training a neural network on a dataset of cryo-EM images labeled with known material properties, the network can learn to identify the unique features associated with different materials or structural characteristics. This training involves feeding the network a large number of images and letting it adjust its internal parameters to minimize the difference between its predictions and the actual data.

Once trained, the neural network can be applied to new, unlabeled cryo-EM images to predict their material properties. This process could revolutionize how scientists understand biological structures, allowing for rapidly categorizing materials based on their visual characteristics. For example, a neural network might learn to distinguish between protein complexes with different mechanical properties or identify the presence of specific materials within a larger cellular structure, all from the visual data provided by cryo-EM.

The process of training a neural network for material property retrieval is a systematic one. It starts with the acquisition of a large and diverse dataset of labeled cryo-EM images. Data augmentation techniques, such as rotating or flipping the images, can help increase the size and variability of the data set, enhancing the network's ability to generalize from its training. The network is then trained by iteratively adjusting its parameters to reduce the difference between its predictions and the true labels of the training images, a process often facilitated by back-propagation algorithms. After training, the network's performance is evaluated on a separate set of test images to ensure it can accurately predict material properties on data it hasn't seen before.

Deploying a neural network trained this way could significantly aid in studying bio-molecules, and allow researchers to infer material properties from cryo-EM images quickly. This could enhance our understanding of the mechanical behavior of bio-molecules in their natural environments, contributing to advances in material science, bio-engineering, and related fields.

1.6 Forward Euler algorithm

In mathematics and computational science, the Euler method (also called the forward Euler method) is a first-order numerical procedure for solving ordinary differential equations (ODEs) with a given initial value. It is the most basic explicit method for numerical integration of ordinary differential equations and is the simplest Runge–Kutta method ("Euler Method for the Cauchy Problem," n.d.).

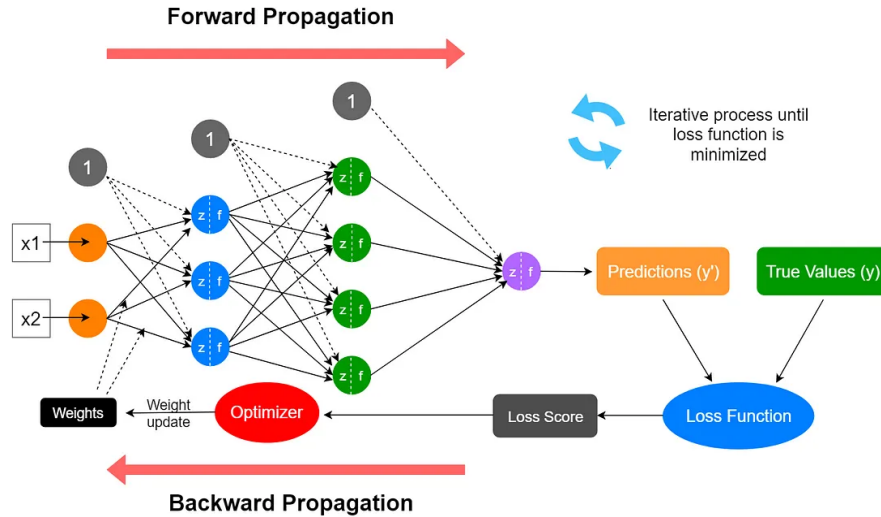


Figure 1.2: Image retrieved from <https://medium.com/data-science-365/overview-of-a-neural-networks-learning-process-61690a502fa>

We're presented with a basic, single-variable ODE

$$\frac{dy}{dt} = f(t, y) \quad (1.1)$$

and we want to predict the behavior of function $y(t)$ over time, starting from an initial state $y(t = 0) = y_0$, to understand how the function $y(t)$ evolves for all times $t > 0$. In particular, we would like to use an algorithm that is able to be executed by a computer to find the evolution of $y(t)$ for all times.

To derive the algorithm, first replace the exact equation with an approximation based on the forward difference derivative to get

$$\frac{y(t + h) - y(t)}{h} \approx f(t, y) \quad (1.2)$$

Now the equation must be discretized. That means we replace our function $y(t)$ defined on continuous t with a sampled function y_n defined on discrete times t_n . That is, $y_n = y(t_n)$. We also imagine the time step between samples is small, $h = t_{n+1} - t_n$. In this case, the previous equation becomes

$$\frac{y_{n+1} - y_n}{h} = f(t_n, y_n) \quad (1.3)$$

Moving forward, we will replace the \approx sign with $=$ for convenience, and keep in mind that behind our expression results in an approximation error which grows with increasing h . Next, imagine we are at the present time point t_n , and rewrite the previous equation to move the future to the left-hand side and the present to the right-hand side. We get:

$$y_{n+1} = y_n + hf(t_n, y_n) \quad (1.4)$$

This expression says that if we know the values of t_n and y_n at the present, then to get the future value y_{n+1} we just perform the computation on the RHS. That is, this equation describes a way to step forward in time. We start at time $t = 0$ with initial condition $y = y_0$ and use the equation to step to y_1 , then use that result to step to y_2 , and y_3 , and so on. By iterating this equation, we generate a vector of y_n values which constitute the sampled version of the function $y(t)$ (Stuart Brorson, in Numerically Solving differential equations).

1.7 Truss model

A truss is a collection of beams joined at nodes, forming a stable framework often used in engineering and architectural design. We can use a simplified truss model comprised of elements and nodes to study the deformation and movements within complex structures, such as proteins, by treating them as a group of rods joined at nodes. This model can be particularly insightful for simulating how proteins respond to the stresses of their environment, including thermal fluctuations. We can use the truss framework to develop a neural network that simulates these interactions and predicts the protein's elasticity and other material properties. The predictions from this neural network, derived from the simulation results or actual data from Cryo-EM imaging, can then be used to train the network further, enhancing its ability to deduce material properties for a protein with unknown material properties. This process will vastly improve our understanding of protein dynamics and flexibility.

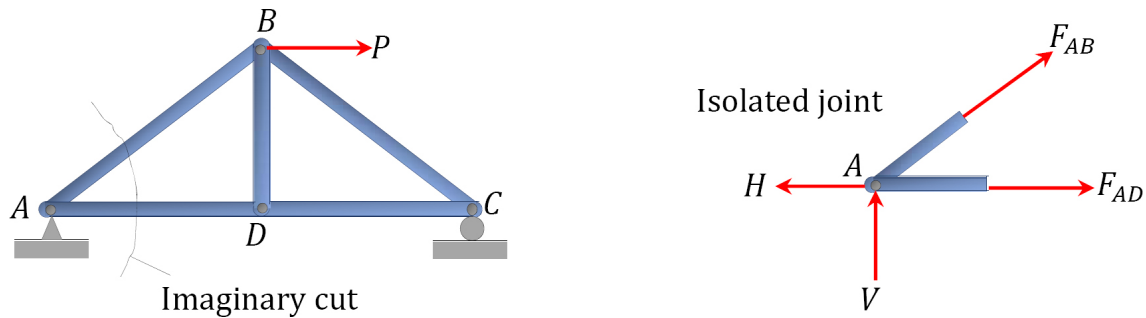


Figure 1.3: A simple truss (Alderliesten, 2022)

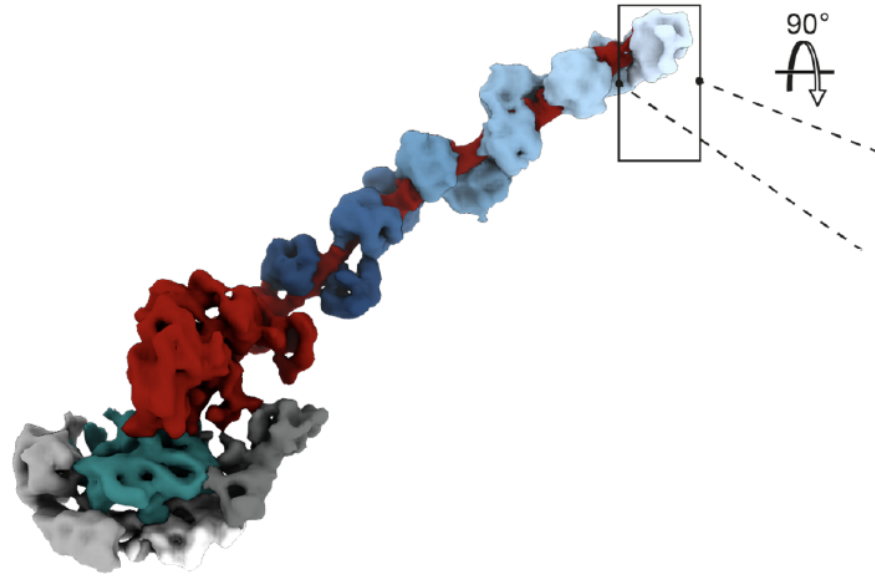
1.8 Ergodic Hypothesis

The ergodic hypothesis is a fundamental concept in statistical mechanics (Lee, M. H., 2002). It asserts that over long periods, the time spent by a system in some region of the phase space of its microstates (or configurations) is proportional to the volume of this region. This implies that time averages and ensemble averages (averages over all possible states of the system) are equivalent for a sufficiently large system or over a sufficiently long time. In simpler terms, given enough time, a system will explore all its possible states, making it possible to understand the system's behavior by examining a long enough sample of its history.

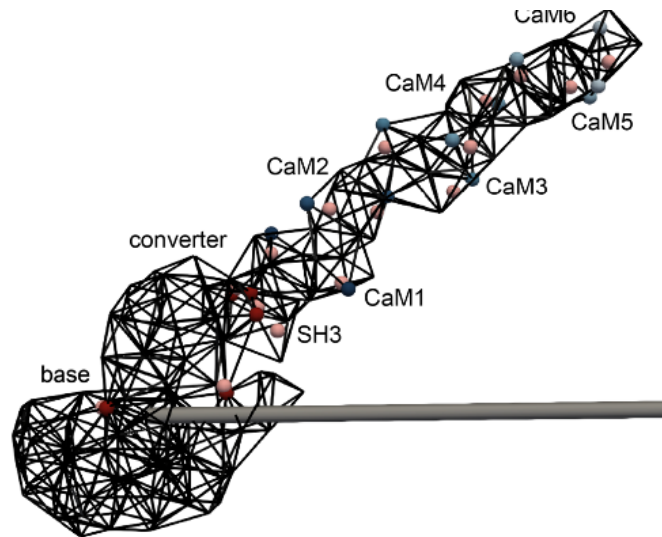
When applied to analyzing truss model displacements, the ergodic hypothesis supports the idea that histograms or statistical distributions derived from long-term observations of node displacements can accurately represent all possible displacement states of the model. By collecting data over time on how the nodes of a truss model move, one can infer the full range of movements the model can undergo. This method of analysis assumes that every potential state will eventually occur, and thus, a long-term observation captures the complete behavior of the system.

Calculating node displacements and matrices of node distances over time provides a statistical distribution of these displacements, allowing for the analysis of the system's behavior in a probabilistic sense. By doing so, one can study the likelihood of specific displacements, offering insights into the structural behaviors under different loads or conditions.

Furthermore, this approach simplifies complex, high-dimensional data into more understandable forms. For example, analyzing extreme eigenvalues and identifying principal modes of displacement can reveal the most significant ways a structure tends to move or deform, shedding light on its mechanical properties and vulnerabilities.



(a)



(b)

Figure 1.4: (a) Cryo-EM map of My05a-S1-6IQ (Gravett, 2022) (b) Nodes in mesh closest to vector coordinates in Cryo-EM model (Gravett, 2022)

The Ergodic hypothesis, therefore, not only justifies the use of statistical methods for analyzing the dynamics of physical systems like truss models but also provides a framework for interpreting these analyses, leading to a deeper understanding of the system's mechanical behavior.

Chapter 2

Procedure

2.1 An Example Truss Model

To explore the possibility of creating data from simulation snapshots of a truss model that could be used to train a neural network for retrieving material properties, I constructed a basic truss model. Figure 2.1 shows this truss in two dimensions and three dimensions respectively.

As mentioned by Welch et al., 2013, the changes to the configuration of the assembly of rod elements is defined by the changes of node positions, Δr_i . The translational motion of each node is given by a stochastic equation of the form:

$$\Delta r_i = \mathcal{M}_i(F_i + f_i)\Delta t. \quad (2.1)$$

In this model, Δt signifies the time step for the simulation, \mathcal{M}_i represents the mobility tensor of a rod segment in a fluid, F_i corresponds to the internal elastic force, and f_i is the stochastic force due to thermal fluctuations. The model operates under the assumption of being highly over-damped, rendering the rod's inertia negligible. Welch et. al (2013) also state that they have neglected the hydrodynamic interactions between the rod elements in equation (2.1), but include a damping force for the motion of an isolated rod element floating in a fluid medium. As a result, this is considered a Brownian equation of motion. For simplicity they have approximated the mobility as being isotropic and equal to the mobility of a sphere of radius a_i , which is half the length at equilibrium of the rod's segment:

$$\mathcal{M}_i = \xi_i^{-1} \mathbf{I}. \quad (2.2)$$

where $\xi_i = 6\pi\mu a_i$ and μ is the dynamic viscosity of the medium.

Using the drag given by equation (2.2), the force acting on each node from thermal noise is given by the fluctuation dissipation theorem (H. Nyquist, 1928):

$$f_i = \sqrt{\frac{24k_B T \xi_i}{\Delta t}} \mathbf{R}. \quad (2.3)$$

where T is the temperature of the system, ξ the friction coefficient, Δt the time step, k_B is the Boltzmann constant, and \mathbf{R} is a random vector, where R_x , R_y , and R_z are independently sampled from a standard normal distribution.

The internal forces within a structure can be quantified using the fundamental principles of material mechanics. The resulting internal force, denoted by F_i , is derived from the stress-strain relationship, which is expressed by the equation:

$$E\varepsilon = \sigma \quad (2.4)$$

where E is the modulus of elasticity, ε is the strain, and σ is the stress. This relationship is commonly referred to as the stress-strain law. From this law, the force can also be described by the equation:

$$EA\varepsilon = \sigma A = F \quad (2.5)$$

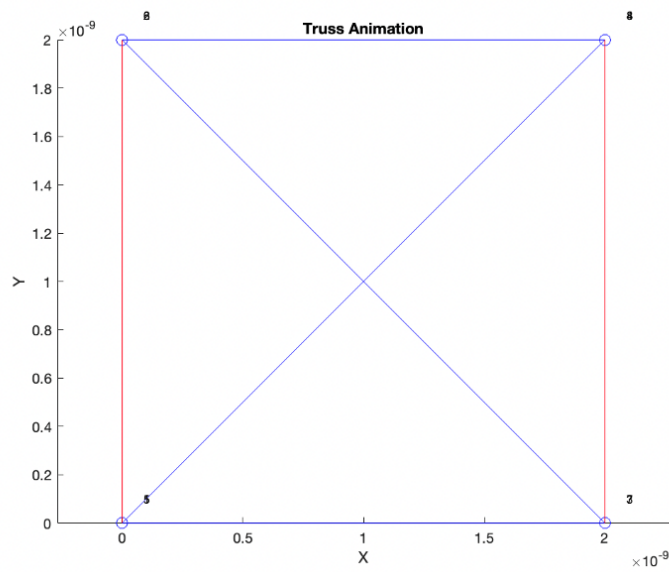
where A denotes the cross-sectional area.

For a specific element, the internal force F_i on each node from that element is given by the relationship:

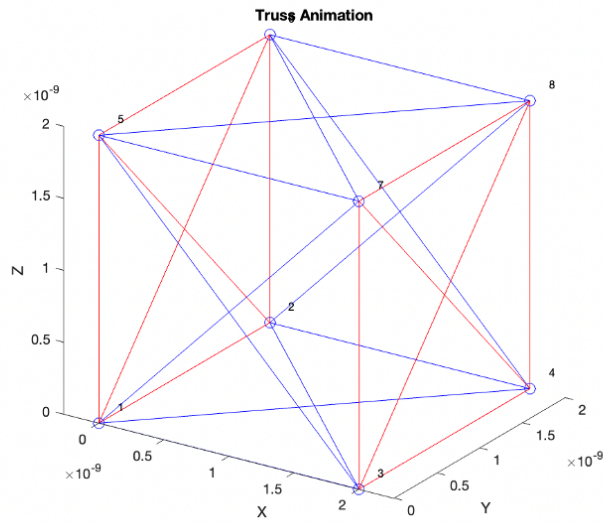
$$F_i = (EA)_{\text{element}} \varepsilon = (EA)_{\text{element}} \frac{\Delta l}{l} \quad (2.6)$$

in which Δl indicates the change in length and l represents the original length. In evaluating Δl , I have considered the exact kinematics of the rods to represent arbitrarily large rotations and elongations.

To reflect variations in structural components, I have assumed different EA parameters assigned based on their location; for example, $(EA)_A$ for elements on the edge and $(EA)_B$ for the inner elements of the truss.



(a)



(b)

Figure 2.1: (a) The simplified Truss structure in 2D. (b) The simplified Truss structure in 3D. The elements colored red have less flexibility than the blue elements. Each data point in a particular histogram corresponds to the two extremal eigenvalues of the all-pairs squared distance matrix of the truss model at a particular time step during simulation. A new data point is inserted in the histogram every 1000 time steps.

2.2 Data Generation

Our study utilized the Forward Euler method to determine the displacements of nodes in our truss model. The time-step was chosen small enough to ensure the stability of the method. This approach allowed for a step-by-step adjustment of node positions to mimic how the truss responds to external forces. Periodically, we created matrices to show the distances between each pair of nodes, providing valuable insight into the truss’s behavior.

These distance matrices were particularly insightful when we examined their extreme eigenvalues. These values revealed the truss’s principal displacement modes. These values showed us the main ways the truss moved, highlighting patterns of movement. Studying these eigenvalues was crucial for predicting how the truss would react to various loading conditions.

The ergodic hypothesis suggests that given enough time, the system will pass through all possible states. This hypothesis allowed us to use histograms to analyze the displacements in the truss model, assuming that long-term observations could accurately represent the entire state space.

The calculation of node displacements and the assembly of node distance matrices provided us with a statistical distribution of displacements over time. By focusing on the analysis of extreme eigenvalues, we could simplify the complex, high-dimensional data into more understandable forms. This approach was helpful in identifying the principal modes of displacement within the truss.

To enhance our understanding of the truss’s behavior, we varied the modulus of elasticity values, $[EA]_A$ for the edge elements and $[EA]_B$ for the inner elements. The resulting histograms for each configuration were systematically catalogued into matrices, which then served as input data for our predictive models. The varied EA values were set as the target outputs. This enables the models to map the relationship between material properties and displacement behaviors.

2.3 The Neural Network

We created a dataset with thousands of data points to encompass a broad spectrum of EA values. Specifically, EA_A , corresponding to the modulus of elasticity for the edge elements of the truss, is consistently larger than EA_B , which pertains to the inner elements. Within our dataset parameters, EA_A is at most ten times greater than EA_B , ensuring a realistic portrayal of the differing mechanical properties across the truss structure.

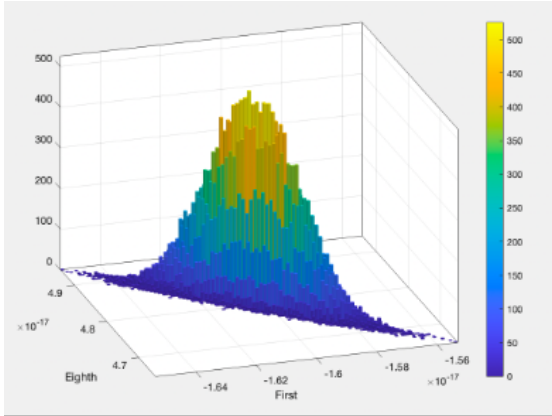


Figure 2.2: EA 1e-5

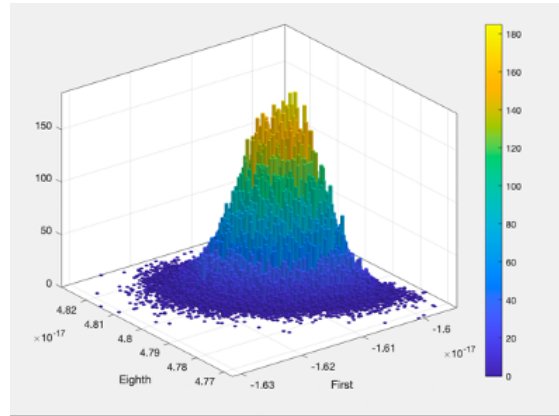


Figure 2.3: EA 1e-6

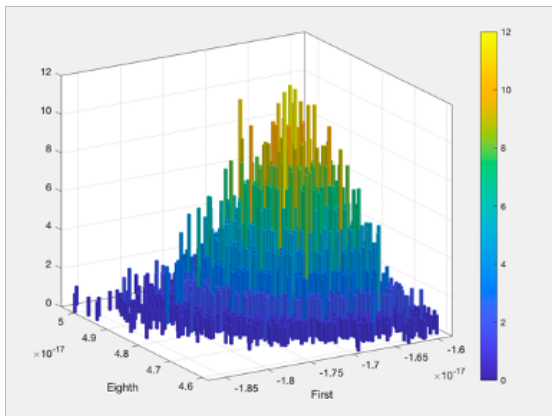


Figure 2.4: EA 1e-8

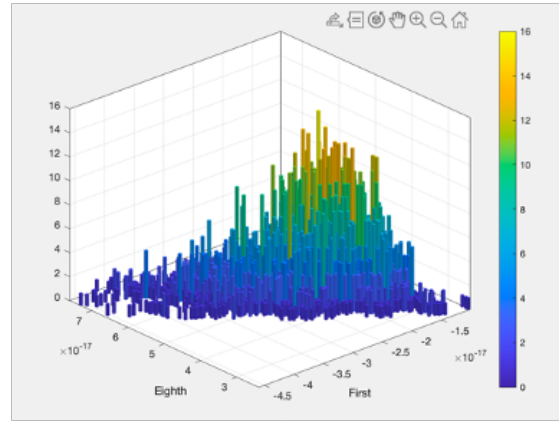


Figure 2.5: EA 1e-9

For our neural network, we used a simple design with just one hidden layer connecting the input and output. To find the best number of neurons for this layer, we tested different amounts with K-fold cross-validation. This method helped us make sure the network would work well no matter the situation.

Additionally, I used L2 regularization in the training to prevent overfitting, which is when a model gets too tuned to the training data and does not do well with new information. This technique helps keep the model flexible.

We chose an optimization method known as Stochastic Gradient Descent with Momentum (SGDM) because it learns fast and smooths out the process.

Lastly, we varied the learning rate during training with a step-by-step method. This let the network learn quickly at first and then more slowly and carefully as it got closer to what we wanted it to do, making the whole training more effective.

2.4 The Training process

The matrices generated from histograms acted as the input to the neural network and the two EA values were the targets that we aimed to predict. We allocated 70 percent of all data to the training set, 15 percent to the validation set, and 15 percent to the test set.

In the pre-processing stage, I cleaned up the data by trimming and removing noise from each matrix. This reduced the size of matrices significantly. Then we turned these matrices into vectors of size 1×888 which is not too big for our neural network to handle.

Training was done through the functions available in MATLAB's Neural Network package. It took 1 minute and 25 seconds for the training process to complete, and it stopped when it reached the validation criterion, which was a tolerance of five. This means that to prevent over-fitting, the training will stop if the validation set loss increases for five consecutive points. The training plot can be seen in the figure in the next page.

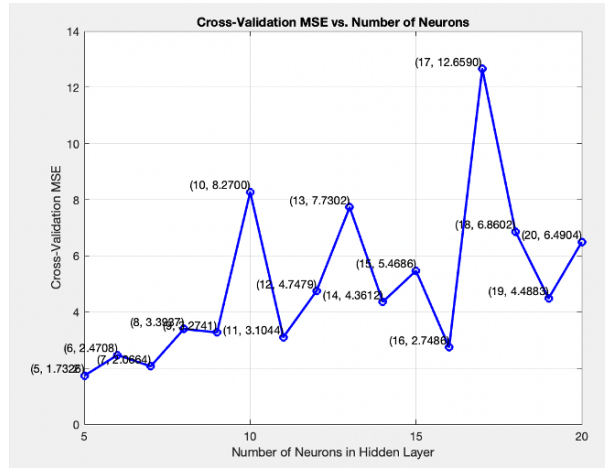


Figure 2.6: Cross validation MSE (Mean Squared Error) to choose the optimum number of neurons of the hidden layer.

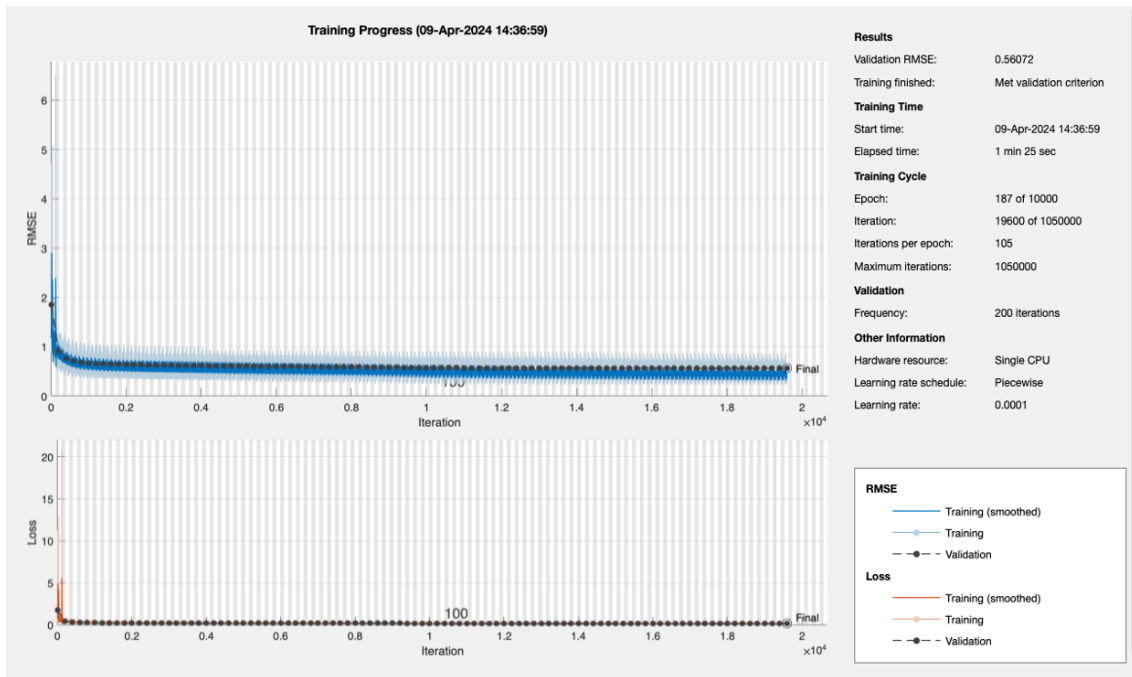


Figure 2.7: The training process with piece-wise learning rate and validation tolerance of 5.

Chapter 3

Results

The neural network's testing phase provided insightful outcomes. The training was concluded successfully when the model met the predetermined validation criteria. The Mean Absolute Error (MAE) was used as a metric to evaluate the model's performance. For the training set, the MAE was recorded at 0.31542134, reflecting the model's average deviation from the actual values. Similarly, the MAE for the test set was slightly higher at 0.33872029, indicating a consistent performance when the model was exposed to unseen data.

To further assess the model's predictive accuracy, we analyzed the test set results in greater detail. A Test R-squared (R^2) value of 0.8866 was achieved, which denotes a high level of correlation between the predicted values and the actual outcomes. This high R^2 value suggests that the model can explain a significant portion of the variance in the test data, which indicates strong predictive capabilities.

A scatter plot of predicted versus actual values graphically illustrates the model's performance, with most points closely aligning with the identity line. This visualization confirms the numerical findings, showing a concentration of predictions around the line of perfect agreement, with one of the targets indicated with red circular points and the other target shown with blue circular points.

In conclusion, the neural network demonstrated a robust ability to predict outcomes with high accuracy, as evidenced by the low MAE and high R-squared value. These results are promising and indicate the model's potential utility in practical applications where predictive precision is paramount.

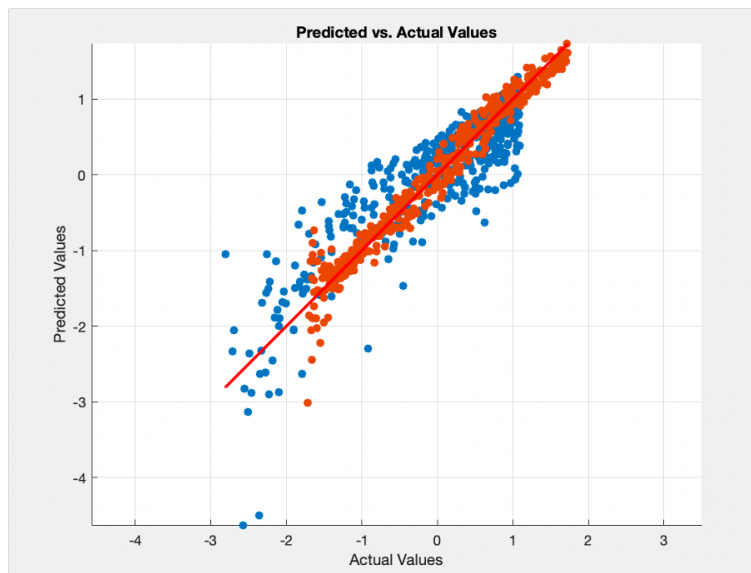


Figure 3.1: The Predicted vs. Actual values of Test data. The blue and red dots show the two targets and the red line shows the line of perfect prediction.

Chapter 4

Future Work

In the field of structural biology, there are exciting opportunities to advance our understanding of bio-molecular structures. Our future research, in collaboration with the University of Leeds, aims to use empirical data to uncover the precise node coordinates of bio-molecules. This work will likely involve using real protein data extracted from cryogenic electron microscopy (Cryo-EM) images to model coordinates, paving the way for a deeper understanding of bio-molecular formations at an atomic scale.

Developing a neural network training process is a central component of the planned research methodology. This process is envisioned to predict the elastic response of bio-molecules to thermal fluctuations. Inter-atomic distances are expected to be determined from simulated high-resolution Cryo-EM imagery, laying the groundwork for accurately mapping spatial relationships within bio-molecular assemblies.

The subsequent step in this future research will involve constructing distance matrices to represent the intricate network of atomic interactions. Computing the eigenvalues of these matrices is projected to yield critical insights into bio-molecules' dynamic behavior and vibrational characteristics.

Utilizing the eigenvalue data, histogram matrices are anticipated to be created as an innovative means to encapsulate complex eigenvalue information. These matrices are expected to be instrumental in training neural networks, enabling the system to discern subtle patterns indicative of bio-molecular elastic behavior.

Our collaborative efforts have the potential to revolutionize the precision of predictive models for bio-molecular structures. By harnessing advanced neural network training techniques and leveraging simulated datasets, we aspire to set new standards in the pre-

dictive modeling of bio-molecular elasticity. This could potentially lead to groundbreaking discoveries in the field of structural biology.

References

- Alderliesten, R. (2022). *Introduction to aerospace structures and materials*. TU Delft Open. Retrieved from [https://eng.libretexts.org/Bookshelves/Mechanical_Engineering/Introduction_to_Aerospace_Structures_and_Materials_\(Alderliesten\)](https://eng.libretexts.org/Bookshelves/Mechanical_Engineering/Introduction_to_Aerospace_Structures_and_Materials_(Alderliesten))
- Borson, S. (2024). *Numerically solving ordinary differential equations*. Boston, MA: Northeastern University. Retrieved from [https://math.libretexts.org/Bookshelves/Differential_Equations/Numerically_Solving_Ordinary_Differential_Equations_\(Borson\)](https://math.libretexts.org/Bookshelves/Differential_Equations/Numerically_Solving_Ordinary_Differential_Equations_(Borson)) (Available under CC BY-SA 3.0 License)
- Bustamante, C., Keller, D. J., & Oster, G. F. (2001). The physics of molecular motors. *Accounts of chemical research*, *34*(6), 412-20. Retrieved from <https://api.semanticscholar.org/CorpusID:7085208>
- Gravett, M. S. C. (2022, December). *Understanding the mechanics of myosin 5a through computational modelling and cryo-em*. Retrieved from <https://etheses.whiterose.ac.uk/32517/>
- Hess, H. (2011). Engineering applications of biomolecular motors [Journal Article]. *Annual Review of Biomedical Engineering*, *13*(Volume 13, 2011), 429-450. Retrieved from <https://www.annualreviews.org/content/journals/10.1146/annurev-bioeng-071910-124644> doi: <https://doi.org/10.1146/annurev-bioeng-071910-124644>
- Lee, M. H. (2002, 11). Boltzmann's Ergodic Hypothesis: Time Averaging and Dynamic Mechanisms. *AIP Conference Proceedings*, *643*(1), 143-148. Retrieved from <https://doi.org/10.1063/1.1523795> doi: 10.1063/1.1523795
- Milne, J. L. S., Borgnia, M. J., Bartesaghi, A., Tran, E. E. H., Earl, L. A., Schauder, D. M., ... Subramaniam, S. (2013). Cryo-electron microscopy – a primer for the non-microscopist. *The FEBS Journal*, *280*(1), 28-45. Retrieved from <https://febs.onlinelibrary.wiley.com/doi/abs/10.1111/febs.12078> doi: <https://doi.org/10.1111/febs.12078>
- Nelson, B. J., Kaliakatsos, I. K., & Abbott, J. J. (2010). Microrobots for minimally

- invasive medicine. *Annual review of biomedical engineering*, *12*, 55-85. Retrieved from <https://api.semanticscholar.org/CorpusID:13639374>
- Purcell, E. M. (1977, 01). Life at low Reynolds number. *American Journal of Physics*, *45*(1), 3-11. Retrieved from <https://doi.org/10.1119/1.10903> doi: 10.1119/1.10903
- Robert-Paganin, J., Pylypenko, O., Kikuti, C., Sweeney, H., & Houdusse, A. (2019, 11). Force generation by myosin motors: A structural perspective. *Chemical Reviews*, *120*. doi: 10.1021/acs.chemrev.9b00264
- Welch, R., Harris, S. A., Harlen, O. G., & Read, D. J. (2020). Kobra: a fluctuating elastic rod model for slender biological macromolecules. *Soft matter*, *16*(32), 7544-7555.